Preparation of graphene oxide–molecularly imprinted polymer composites via atom transfer radical polymerization

Limin Chang · Shu Wu · Shaona Chen · Xin Li

Abstract A molecularly imprinted polymer–graphene oxide hybrid material was synthesized by atom transfer radical polymerization. The formation of this hybrid material was verified by Raman spectroscopy and energy dispersive spectrum. Transmission electron microscopy and atomic force microscopy showed that the average thickness of the imprinted polymer grafted on the surface of graphene oxide is about 10.957 nm. Moreover, the hybrids bind the original template 2,4-dichlorophenol with an appreciable selectivity over structurally related compounds. In addition, the method could lead to further development of graphene-based nanoelectronics.

Introduction

Graphene-based hybrid materials have been attracted a great deal of attention due to their promising applications in fields such as catalysis, biosensors, and nanoelectronic devices [1, 2]. Up to date, diverse methods for the functionalization of graphene have been developed [3–14]. However, it is difficult to control and quantify the functionality, density, and thickness of grafted materials [15]. Thus, it is still a challenge to prepare graphene-based composite.

In this study, molecularly imprinted polymer (MIP) is introduced as the functionalizing material for graphene oxide (GO). Molecular imprinting is already a highly accepted tool for the preparation of tailor-made recognition material, and allows the creation of synthetic receptors with higher affinity and specificity [16–20]. We have successfully synthesized MIP–GO hybrid material by reversible addition and fragmentation chain transfer polymerization [21]. In this article, GO were first functionalized with initiator of atom transfer radical polymerization (ATRP), and then MIP were grown directly via a surface-initiated polymerization. Since its first discovery in 1995 [22], ATRP has been shown to be one of the most successful controlled "living" radical polymerization methods. Surface-initiated ATRP allows the preparation of polymers with interesting functionalities and architectures. Recently, ATRP has been used in generation of MIPs with improved properties [23–27]. ATRP also has been used in modifying the surfaces of silica [28–30], gold [31], nanoparticles [32–34], biomaterial [35, 36], carbon nanotube [37, 38], and graphene [39, 40].

The route to synthesize the GO–MIP is shown schematically in Scheme 1. In this study, 2,4-dichlorophenol (2,4-DCP) was chosen as a model analyte, because it is an estrogen mimic commonly detected in the natural environment. To the best of our knowledge, it is the first study to synthesize GO–MIP hybrid material using ATRP. We believe that our study paves a way to the synthesis of graphene-based hybrid materials possess wide applications in different fields.

L. Chang · S. Chen
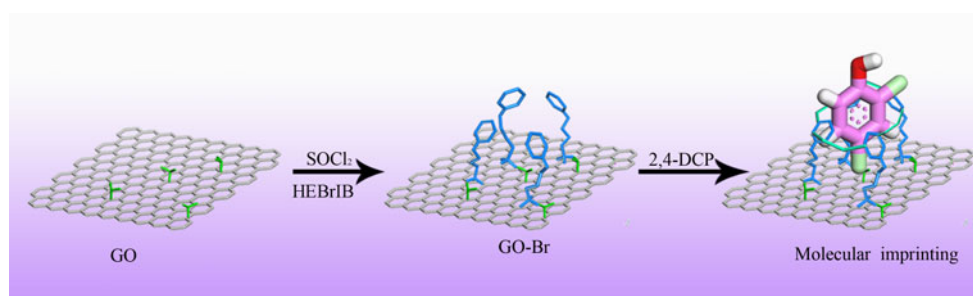Analysis and Measure Center, Jilin Normal University,
Siping 136000, China

S. Wu · X. Li (✉)
State Key Lab of Urban Water Resource and Environment,
Department of Chemistry, Harbin Institute of Technology,
Harbin 150090, China
e-mail: lixin@hit.edu.cn

Experimental

Preparation of GO–MIP hybrid

GO was first prepared according to the modified Hummers method [41]. 2-Hydroxylethyl-2′-bromoisobutyrate

Scheme 1 Schematic diagram of GO–MIP synthesis using ATRP

(HOCH$_2$–CH$_2$OCOC(CH$_3$)$_2$Br, HEBrIB) was then prepared using a previously reported method [42]. ^{1}H NMR (δ, ppm), 1.04(s, 6H, 2-CH_3), 3.56 (t, 2H, OCH$_2$$CH_2$OH), 4.34 (t, 2H, –COO$CH_2$–CH$_2$–).

In a typical experiment, 1.0 g of GO was dispersed in 100.0 mL of SOCl$_2$ and 20.0 mL of benzene. The mixture was stirred for 24 h under 70 °C at reflux. The obtained solid (GO–Cl) was washed with ultra-dried tetrahydrofuran (THF) three times and dried under vacuum at 25 °C. In the next step, GO–Br was prepared using a previously reported method [21]. Subsequently, 113 mg 2,4-dichlorophenol (2,4-DCP, template), 510 mg methacrylamide (MAAM), and 4.3 mL divinylbenzene (DVB) were dispersed into a 13 mL acetonitrile solution, and the mixture was stirred for 1 h. After sealing, shaking, and purging the mixture with 70 mg GO–Br, 44 μL N,N,N',N',N''-pentamethyldiethylenetriamine (PMDETA), and 28.6 mg CuBr was added under nitrogen protection at 65 °C for 18 h. The polymerization was stopped by freezing. The obtained product separately washed three times with acetone and methanol–acetic acid (9:1, v/v) solution to remove the catalyst and unreacted reagents. Finally, the resultant product was dried under vacuum at room temperature for 24 h.

Characterization

The samples were characterized by transmission electron microscopy (TEM, TECNIG20, 200 kV), atomic force microscopy (AFM, Digital Instrument NanoscopeIIIa, in tapping-mode), energy dispersive spectrum (EDS, EDAX-PHOE-NIX), and Raman spectrometer (Jobin–Yvon HR 800, with laser excitation at 457.9 nm.). ^{1}H nuclear magnetic resonance (NMR) spectra were analyzed on a Bruker Avance-300 instrument with CDCl$_3$ as solvent.

Competitive adsorption

Phenol and 4-monochlorophenol were chosen as competitive agents since their chemical molecular structures are similar to 2,4-DCP to a certain extent. 8.5 mg GO–MIP hybrid was dispersed in 5.0 mL of aqueous solutions containing different concentrations (10, 24.5, and 50 mg L^{-1})

of 2,4-DCP, 4-monochlorophenol, and phenol, respectively. The mixture was shaken in HY Vertical multi-purpose Vibrator at 25 °C for 4 h. The concentration of 2,4-DCP (i.e., phenol and 4-monochlorophenol) was determined using HP1100 (Agilent) high performance liquid chromatograph (HPLC) with a UV–vis detector.
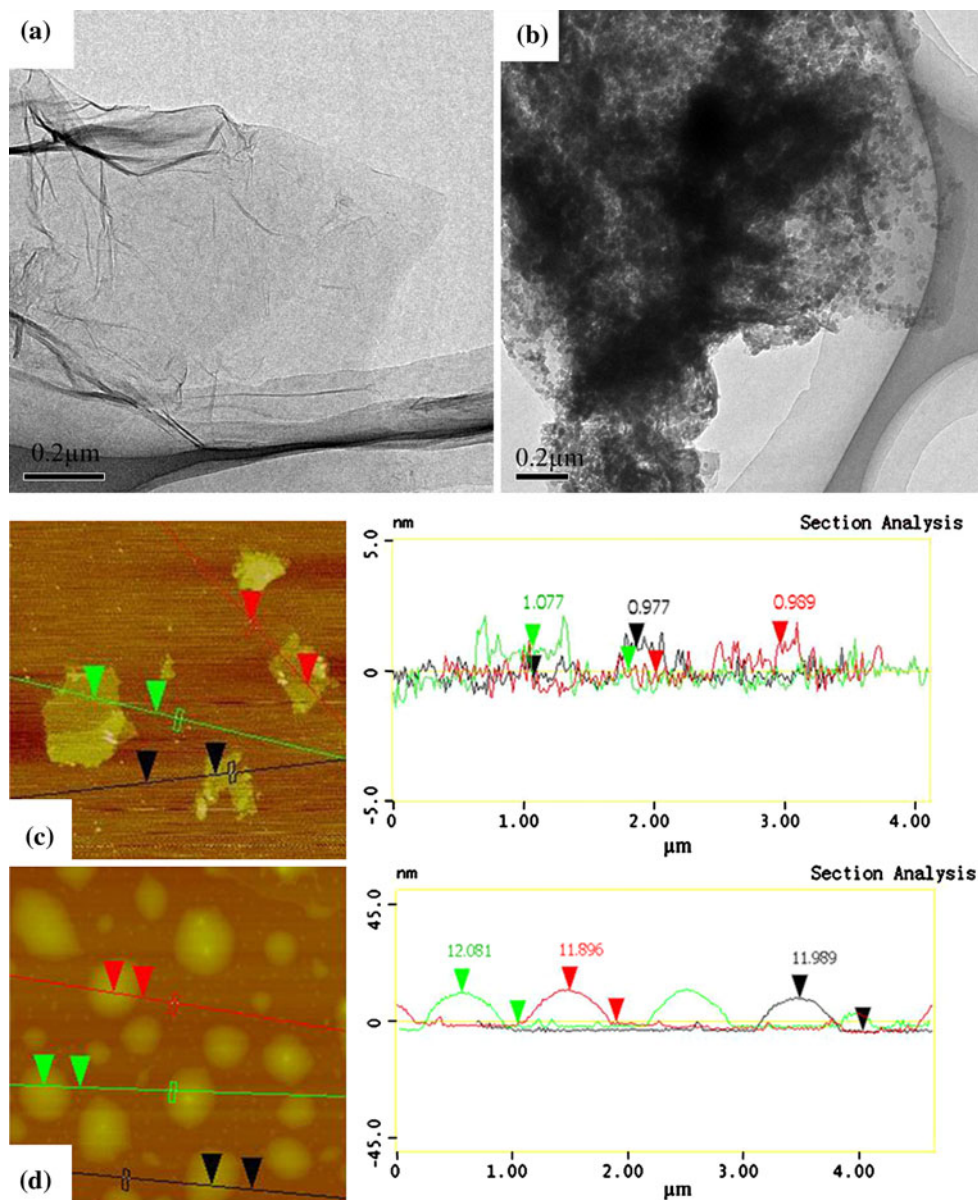
Results and discussion

The morphology of the GO–MIP hybrid was characterized with TEM and AFM. As can be seen from the TEM image, the morphology of GO is very thin and contains some folds and crinkles (Fig. 1a).These crinkles may be important for preventing aggregation of GO and maintaining high surface area [43]. The TEM image of the GO–MIP hybrid shows the presence of grafted polymer on GO surfaces (Fig. 1b). From the image of AFM (Fig. 1c), GO shows a height of around 1.014 nm, suggesting a single-layer nanosheets. From the AFM height analysis in Fig. 1d, the average thickness of the polymer grafted on the GO surface is about 10.975 nm.

The existence of MIP-coatings was further confirmed by the EDS analysis. In Fig. 2a, the signal of oxygen and carbon appeared for GO. The structure of GO–Cl was further supported by the observation of EDS spectrum from the emergence of Cl signal (Fig. 2b). As shown in Fig. 2c, it was observed that a new signal of Br appeared due to the immobilization of HEBrIB onto the surface of GO. Emergence of N signal in Fig. 2d provides an additional evidence for the presence of grafted polymer.

Further evidence of bonding between GO and MIP is provided by the FT-IR spectra shown in Fig. 3. In the spectrum of GO–MIP, the peak at 3030 cm^{-1} is the N–H bending band, and the peak at 1161 cm^{-1} is characteristic of the C–N stretch of acid amide, which confirms the presence of grafted polymers on the GO.

The interaction between MIP and GO was investigated by using Raman spectroscopy (Fig. 4). Raman spectroscopy is a powerful tool for characterizing carbonaceous materials because of their high Raman intensities [44]. As shown in Fig. 4, the Raman spectrum of GO exhibited a

Fig. 1 TEM images of (**a**) GO and (**b**) GO–MIP. Tapping-mode AFM images of (**c**) GO and (**d**) GO–MIP dispersion dip-coated on mica

D-band peak at 1366 cm^{-1} due to the double-resonance excitation of phonons close to the K point in the Brillouin zone, and a G-band peak at 1582 cm^{-1} that corresponds to the Brillouin zone-centered LO-phonon [45, 46]. In general, the D-band assigned to the sp^3 carbons in graphene sheets, and the D mode of GO is relatively weak due to the symmetry breaking at the edge. In carbonaceous material, G-band in the Raman spectrum corresponds to sp^2 carbon stretching modes [47]. Besides, the intensity ratio (I_D/I_G) is characteristic of the extent of disorder present within in the material [48, 49]. Upon calculation, the I_D/I_G ratios of the GO, GO–Br, and GO–MIP are, respectively, 0.670, 0.884 and 1.169, reflecting the increase in disorder. The change in the I_D/I_G ratio can be at least partly attributed to the formation of covalent bonds between graphene and

initiator and/or MIP [50]. By comparing the G-bands of GO and GO–MIP, it is clear that G-band of GO–MIP occurs at 1574 cm^{-1}, which is downshifted by 8 cm^{-1} compared to that of GO. The Raman shifts of the G-band for GO–MIP provide evidence for the charge transfer between the GO sheets and MIP, which suggests a strong interaction between the MIP and the GO sheet [51].

Recognition selectivity is one of the most important parameters in characterizing MIP. Competitive adsorption of 2,4-DCP, phenol, and 4-chlorophenol were studied in a batch system. Phenol and 4-chlorophenol were selected as potential interferents due to their chemical molecular structures which are similar to 2,4-DCP to a certain extent. It can be seen clearly that the GO–MIP exhibits significantly lower binding capacities toward 4-chlorophenol and
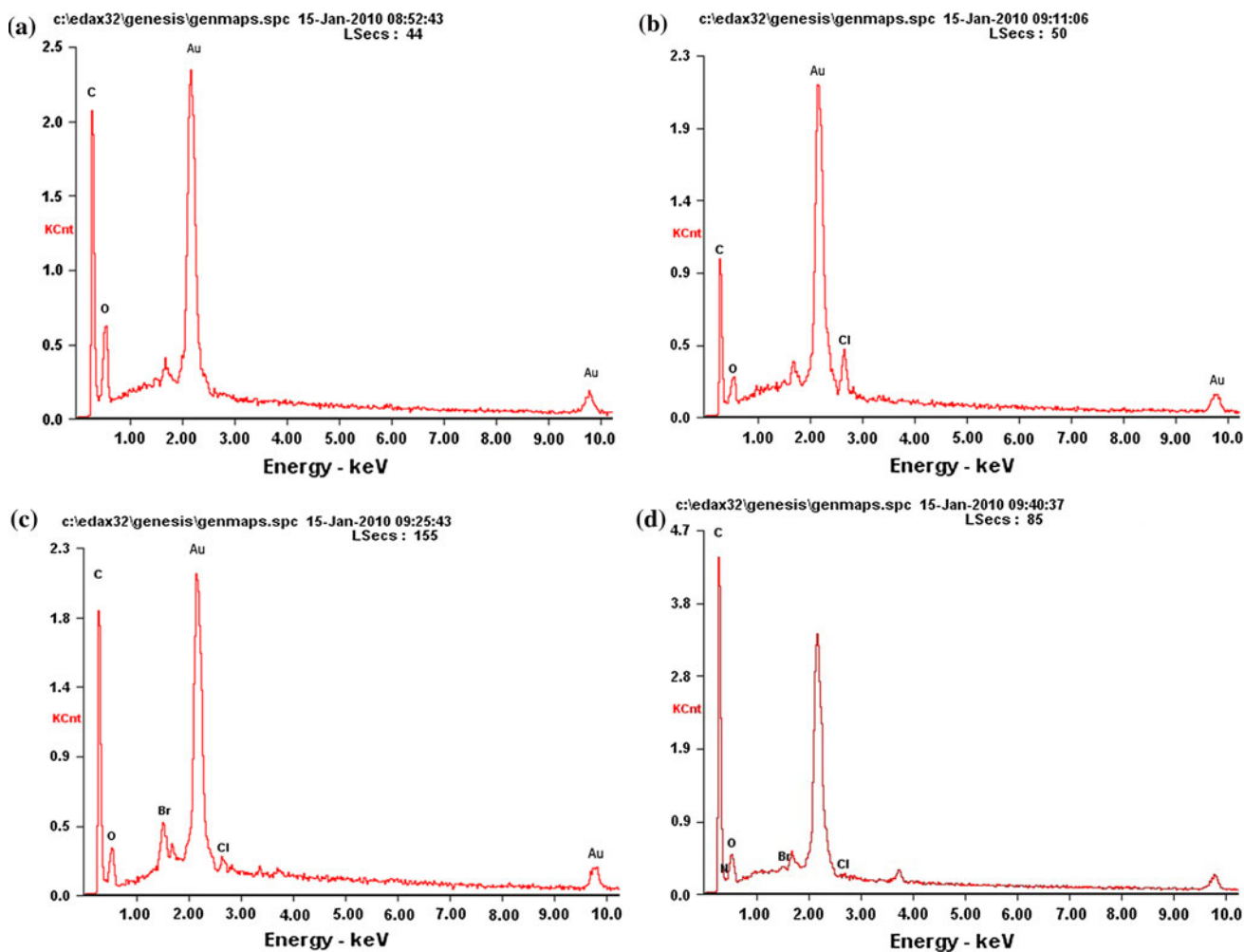
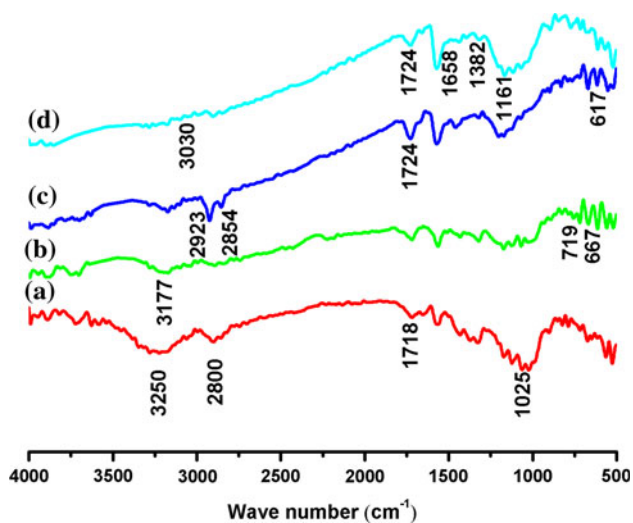Fig. 2 EDS spectra of **a** GO, **b** GO–Cl, **c** GO–Br, and **d** GO–MIP

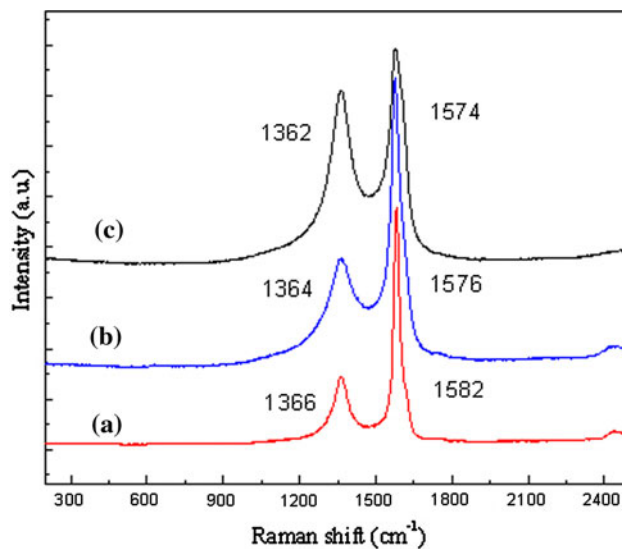Fig. 3 FT-IR spectra of (*a*) GO, (*b*) GO–Cl, (*c*) GO–Br, and (*d*) GO–MIP

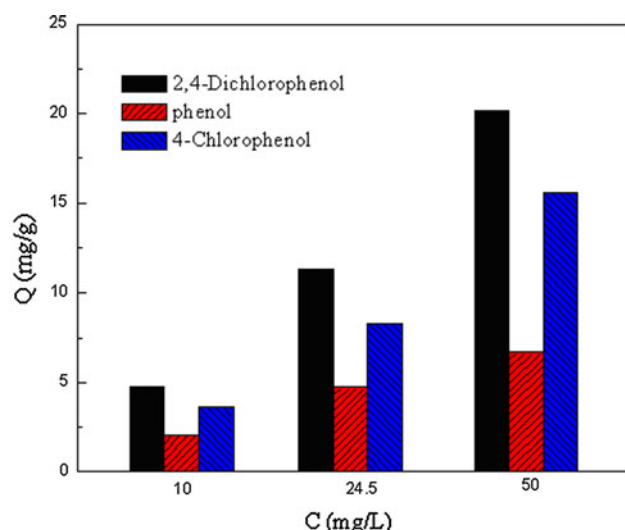Fig. 4 Raman spectra of (*a*) GO, (*b*) GO–Br, and (*c*) GO–MIP

Fig. 5 The cross reactivity of the GO–MIP for adsorption of 2,4-DCP and interferents in aqueous medium

phenol than 2,4-DCP; thus, demonstrating the high selectivity of the GO–MIP toward 2,4-DCP (Fig. 5). Our previous study reported that potential interferents cannot form binding as strong as template, for their size cannot match the imprinting cavities or their functional group position do not correspond to functional groups in imprinting cavities, and thus, cannot bring about specific binding same as template [52]. There is a further possible explanation for the selectivity of the GO–MIP for 2,4-DCP over the analogs. Graphene is a strictly two-dimensional material and, as such, has its large surface area, which provides a complete removal of templates and a very high rebinding capacity. Graphene provides a confined environment to promote higher affinity and sensitivity for target analyte, and a more homogeneous distribution of recognition sites. Furthermore, the transfer of electrons between the π orbitals of graphene and 2,4-DCP, and the formation of π–π stacking, presented synergetic effect on the GO–MIP hybrids.

Conclusions

Summing up, we have demonstrated that GO-based MIP composites can be prepared via controlled "living" radical polymerization, the first experimental example of the grafting of MIP from the surface of GO using ATRP technique. TEM and AFM morphology, EDS, and Raman spectrum were used to demonstrate the successful attachment of MIP to GO sheets. We believe that the effective method described in this article might promote the practical applications of GO-based composites in nanoelectronics.

References

1. Stankovich S, Dikin DA, Dommett GHB, Kohlhaas KM, Zimney EJ, Stach EA, Piner RD, Nguyen ST, Ruoff RS (2006) Nature 442:282
2. Ramanathan T, Abdala AA, Stankovich S, Dikin DA, Herrera-Alonso M, Piner RD, Adamson DH, Schniepp HC, Chen X, Ruoff RS, Nguyen ST, Aksay IA, Prud'Homme RK, Brinson LC (2008) Nat Nanotechnol 3:327
3. Blake P, Brimicombe PD, Nair RR, Booth TJ, Jiang D, Schedin F, Ponomarenko LA, Morozov SV, Gleeson HF, Hill EW, Geim AK, Novoselov KS (2008) Nano Lett 8:1704
4. Eda G, Chhowalla M (2009) Nano Lett 9:814
5. Pasricha R, Gupta S, Srivastava AK (2009) Small 5:2253
6. Wang XR, Tabakman SM, Dai H (2008) J Am Chem Soc 130:8152
7. Muszynski R, Seger B, Kamat PV (2008) J Phys Chem C 112:5263
8. Xu C, Wang X (2009) Small 5:2212
9. Zhou XZ, Huang X, Qi X, Wu SX, Xue C, Boey FYC, Yan QY, Chen P, Zhang H (2009) J Phys Chem C 113:10842
10. Scheuermann GM, Rumi L, Steurer P, Bannwarth W, Mülhaupt R (2009) J Am Chem Soc 131:8262
11. Yang XY, Zhang XY, Ma YF, Huang YS, Wang YS, Chen Y (2009) J Mater Chem 19:2710
12. Li FH, Yang HF, Shan CS, Zhang QX, Han D, Ivaska A, Niu L (2009) J Mater Chem 19:4022
13. Yang HF, Li FH, Shan CS, Han DX, Zhang QX, Niu L, Ivaska A (2009) J Mater Chem 19:4632
14. Li FL, Song JF, Yang HF, Gan SY, Zhang QX, Han DX, Ivaska A, Niu L (2009) Nanotechnology 20:455602
15. Lee SH, Dreyer DR, An J, Velamakanni A, Piner RD, Park S, Zhu Y, Kim SO, Bielawski CW, Ruoff RS (2010) Macromol Rapid Commun 31:281
16. Haupt K, Mosbach K (2000) Chem Rev 100:2495
17. Mahony JO, Nolan K, Smyth MR, Mizaikoff B (2005) Anal Chim Acta 534:31
18. Karim K, Breton F, Rouillon R, Piletska EV, Guerreiro A, Chianella I, Piletsky SA (2005) Adv Drug Deliv Rev 57:1795
19. Yun YH, Shon HK, Yoon SD (2009) J Mater Sci 44:6206. doi: 10.1007/s10853-009-3863-3
20. Wang Z, Wu G, Wang M, He C (2009) J Mater Sci 44:2694. doi: 10.1007/s10853-009-3353-7
21. Li Y, Li X, Dong C, Qi J, Han X (2010) Carbon 48:3427
22. Wang JS, Matyjaszewski K (1995) Macromolecules 28:7572
23. Wei X, Li X, Husson SM (2005) Biomacromolecules 6:1113
24. Li X, Husson SM (2006) Biosens Bioelectron 22:336
25. Wei X, Husson SM (2007) Ind Eng Chem Res 46:2117
26. Zu B, Pan G, Guo X, Zhang Y, Zhang H (2009) J Polym Sci A 47:3257
27. Zu B, Zhang Y, Guo X, Zhang H (2010) J Polym Sci A 48:532
28. Pyun J, Kowalewski T, Matyjaszewski KS (2003) Macromol Rapid Commun 24:1043
29. Chen R, Feng W, Zhu S, Botton G, Ong B, Wu Y (2006) J Polym Sci A 44:1252
30. Sha K, Li DS, Li Y, Wang S, Wang J (2007) J Mater Sci 42:4916. doi:10.1007/s10853-006-0397-9
31. Kim JB, Bruening ML, Baker GL (2000) J Am Chem Soc 122:7616

32. Chen R, Maclaughlin S, Botton G, Zhu S (2009) Polymer 50:4293
33. Vestal CR, Zhang ZJ (2002) J Am Chem Soc 124:14312
34. Cui T, Zhang J, Wang J, Cui F, Chen W, Xu F, Wang Z, Zhang K, Yang B (2005) Adv Funct Mater 15:481
35. Kim YS, Kadla JF (2010) Biomacromolecules 11:981
36. Xu FJ, Wang ZH, Yang WT (2010) Biomaterials 31:3139
37. Baskaran D, Mays JM, Bratcher MS (2004) Angew Chem Int Ed 43:2138
38. Choi WS, Ryu SH (2010) J Appl Polym Sci 116:2930
39. Yang Y, Wang J, Zhang J, Liu J, Yang X, Zhao H (2009) Langmuir 25:11808
40. Fang M, Wang K, Lu H, Yang Y, Nutt S (2010) J Mater Chem 20:1982
41. Hummers WS, Offeman RE (1958) J Am Chem Soc 80:1339
42. Hong CY, You YZ, Pan CY (2005) Chem Mater 17:2247
43. Schniepp HC, Li JL, McAllister MJ, Sai H, Herrera-Alonso M, Adamson DH, Prud'homme RK, Car R, Saville DA, Aksay IA (2006) J Phys Chem B 110:8535
44. Ferralis N (2010) J Mater Sci 45:5135. doi:10.1007/s10853-010-4673-3
45. Kotov NA, Dekany I, Fendler JH (1996) Adv Mater 8:637
46. Thomsen C, Reich S (2000) Phys Rev Lett 85:5214
47. Ferrari AC, Robertson J (2000) Phys Rev B 61:14095
48. Choi WS, Choi SH, Hong B, Lim DG, Yang KJ, Lee JH (2006) Mater Sci Eng C 26:1211
49. Kudin KN, Ozbas B, Schniepp HC, Prud'homme RK, Aksay IA, Car R (2008) Nano Lett 8:36
50. Fang M, Wang K, Lu H, Yang Y, Nutt S (2009) J Mater Chem 19:7098
51. Manna AK, Pati SK (2009) Chem Asian J 4:855
52. Li Y, Li X, Li Y, Dong C, Jin P, Qi J (2009) Biomaterials 30:3205